Summary Report on Innovative Detector Ideas

Randal C. Ruchti
Department of Physics
University of Notre Dame
Notre Dame, Indiana 46556

The general theme of the detector group has been to consider innovative and speculative ideas in experimental instrumentation and to identify fruitful approaches in instrumentation for the future. Specifically we have tried to identify general characteristics of detectors needed for various experiments and to establish ultimate limitations for various techniques. No attempt has been made to design overall detectors, nor have we attempted to be comprehensive.

The detector group was subdivided into the following working groups:

1. High spatial resolution vertex detectors;
   Bulos, Kagen, Lipton, Martin, Nygren, Platner, Ruchti, Sticker, Thornton
2. Calorimetry;
   Abolins, Herb, Pauss, Tuts, Vogel
3. Particle identification;
   Olsen, Reibel, Platner
4. Electrodeless drift chambers;
   Ayres, Tzanakos
5. High luminosity considerations;
   Platner
6. Speculative ideas;
   Olsen, Ruchti.

It is the purpose of this presentation to review some of the highlights from each of the working groups. For further detail the reader is referred to specific contributions of group members which appear in these proceedings.

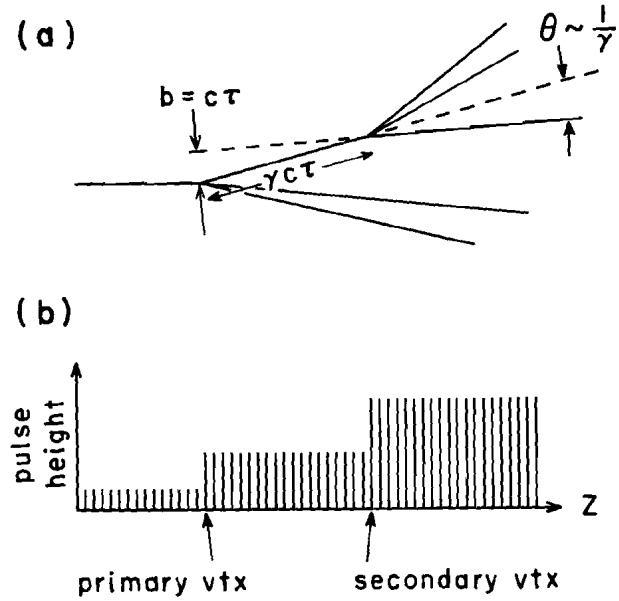

Figure 1. Schematic of a particle decay downstream of a primary interaction vertex as seen in:
(a) an optical device such as a bubble chamber;
(b) an ionization sampling device such as a stack of Si wafers.

1. High Spatial Resolution Vertex Detectors

This subgroup placed its emphasis on the detection of decays-in-flight of short-lived particles. The range of particle lifetimes under consideration has been:

Lifetime (sec)	Effective Impact Parameter	Particle
10^{-12}	300 μm	$D^{\pm}$
10^{-13}	30 μm	D^{0}, $\Lambda_c^{\pm}$, $F^{\pm}$, $\tau^{\pm}$
10^{-14}	3 μm	B, Λ_B
$<10^{-16}$	< .03 μm	T, Λ_T

The experimental techniques to identify decays-in-flight include: direct reconstruction of a decay vertex; detection of a finite impact parameter for secondary tracks at the primary vertex; and observation of a discrete change in ionization as a function of distance. How each of these techniques can be applied is illustrated in Figure 1, which indicates schematically a particle decay. Direct reconstruction of decay vertices and finite impact parameter analyses have been accomplished conventionally in optical devices such as a rapid-cycling bubble chamber or emulsion plate, or by track reconstruction using high resolution chambers. With the development of silicon micro-strip detectors, it is possible to impose a finite impact-parameter requirement at the trigger level. Ionization change techniques can identify the longitudinal distance from the primary interaction point at which a weak decay occurs, by looking for discrete changes in detected charge associable to charged decay secondaries. Since silicon wafers are used for the ionization measurements, such devices could also be included in trigger decisions.

The charm system is already being studied using combinations of the above techniques. However to detect lifetimes of $\tau \gtrsim 10^{-14}$ sec (a range important for B decays) will require detectors which provide for a spatial resolution of $\sigma \lesssim 10\ \mu m$ per point and sufficiently frequent measurements of this resolution size to overcome the effects of multiple scattering. As an example, suppose one is interested in meas-

uring a lifetime of $\tau \sim 10^{-14}$ sec, for which $C\tau$ is $3\mu m$. Assuming that a 3σ measurement of the impact parameter is sufficient to identify a decay secondary, one must be able to measure impact parameters of order $1\,\mu m$ in an active target system. In Table I is indicated the number of measurements of $\sim 10\,\mu m$ resolution per centimeter of track length in bulk material to achieve the requisite resolution in impact parameter; a particle momentum of 10 GeV/c has been assumed. As revealed by the table, targets composed of higher Z materials require more detected hits per unit length because of increased multiple scattering. Propane or hydrogen bubble chambers and emulsion plates all realize the required hit density.

TABLE I

Target Material	Hits/cm Required
Si	80
Ge	166
Propane	37
Hydrogen	18
Emulsion	125

The number of detected hits/cm in bulk material required for a 10 GeV/c charged particle, with resolution $\sim 10\,\mu m$/hit, in order to resolve an impact parameter of $1\mu m$(after R. Lipton in these proceedings).

However it is interesting to note that silicon strip detectors do not satisfy the above criterion. These devices are typically $300\,\mu m$ thick in order to obtain a useful signal. Even with the densest possible packing, these detectors can provide a hit density of only 30/cm which is insufficient for measurements of impact parameter of order $1\,\mu m$.

We summarize in Table II the properties of a large number of vertex detectors, some tried-and-true, some presently under development, some speculative, some wildly speculative. Which detector is appropriate in a given experimental configuration depends not only on spatial resolution, but also on beam-rate capability and whether or not the device is triggerable/gatable. A particularly interesting set of targets are those for which a storage and gating capability exists. The photo-image of the interaction in the active target material is stored on an intermediate phosphor stage of a multi-stage image intensifier. When an appropriate experimental trigger condition is satisfied, the stored image can be gated onto the readout stage of the device. The data recording medium can be film, vidicon, CCD, etc. (See paper by R. Ruchti on Scintillating Glass Fiber-Optic Targets in these proceedings.) Such devices are capable of relatively high beam rates, and can be used in conjunction with sophisticated triggering schemes.

In terms of looking for decays-in-flight of high mass particle states, fixed target experiments are an excellent choice for several reasons: first, γ factors for outgoing particles are large ($\gamma_{cms} \sim 100$ for a 20 TeV/c beam on a fixed target) and as a consequence, momenta for secondaries are stiff; second, one can put an active target directly into the beam; third, one does not have beam pipes in the way to multiple scatter outgoing tracks. Potential drawbacks for a fixed-target program are the relatively low center-of-mass energy ($\sqrt{s}$) available vis-a-vis colliders and the possibility of secondary interactions of outgoing tracks in target materials (a problem which must be considered for very high energy).

The group has also examined the outlook for combining high-resolution detectors into experiments at e^+e^- colliders. Following an analysis by Kagen and Bulos, an interaction region (Figure 2) was assumed to be instrumented with two layers of silicon microstrip detectors in the vicinity of the beam pipe.

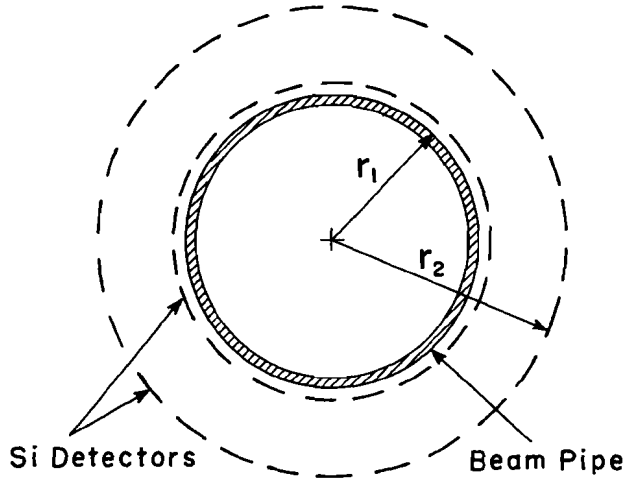

Figure 2. Schematic of an intersection region at a collider which is instrumented with silicon microstrip detectors at radii r_1 and r_2. (Viewed along the beam direction.)

The inner Si detector was assumed to be placed right against the beam pipe at radius r_1; the outer detector position r_2 was allowed to vary. For given assumptions about beam pipe radii and radiation lengths for typical materials used to make beam pipes (see Table III), the measurement resolution at an extrapolated decay vertex was determined as a function of the parameter $a = r_1/r_2$. Calculationally the resolution was determined as follows. For a given detector plane, the following quantities were defined:

$\sigma_I(i)$ = inherent resolution for plane i. (typically $10\,\mu m$ for silicon strip detectors)

$\sigma_{MS}(i)$ = multiple scattering resolution at plane i. (For plane i = 1 at radius $r_1 = 1$ cm, $\sigma_{MS}(1) \simeq 0$, whereas for plane i = 2, $\sigma_{MS}(2) = C(r_2 - r_1)^2$, where $C = (.015/p\beta)t$ and t is the combined radiation length of the beam pipe wall and inner silicon detector.)

$\sigma(i) = \sqrt{\sigma_I^2(i) + \sigma_{MS}^2(i)}$ = net resolution at i.

TABLE II

A Comparison of Several High Resolution Detectors
(*indicates effective time constant is controlled by image intensifier phosphors)

Detector	Flux/sec	Resolving Time (RT)	Live Time (LT)	Resolution per Point	Hit Density	Two Track Resolution	Comment
Bubble Chamber (Conv. Optics)	10^2	100 μ sec	1-2 m sec	10-30 μm	Few hundred/cm	50 μm	ungatable/untriggerable
Bubble Chamber (Holography)	10^3	100 μ sec	1-2 m sec	3-10 μm	Few hundred/cm	25 μm	ungatable/untriggerable
High Resolution Drift Chamber	10^6	$\lesssim$5 sec	50 n sec	100 μm	1/cm	1 mm	resolution can improve at high pressure
High Resolution PWC	10^6	$\lesssim$5 n sec	20 n sec	$\lesssim$0.5 mm	1/cm	2 mm	
Silicon Strip	10^6	10 n sec	50 n sec	10 μm	25/cm	120 μm	live time depends on pulse shaping
Streamer Chamber	10^4 - 10^5	Few μ sec*	= RT	$\lesssim$100 μm	Few hundred/cm	250 μm	device is triggerable/gatable
Emulsion	---	---	Infinite	$\lesssim$1 μm	2000/cm	3 μm	
Microchannel Plate	10^6	Few μ sec*	= RT	10 μm	20/cm	50 μm	device is triggerable/gatable
NaI Camera	$\gtrsim 10^5$	$\tau_{NaI} \simeq 200$ n sec τ_{eff} = few μ sec*	= RT	20 μm	30/cm	40 μm	device is triggerable/gatable
Scintillating Glass, Fiber-Optic Target	$\gtrsim 10^5$	$\tau_{glass} \simeq 80$ n sec τ_{eff} = few μ sec*	= RT	$\lesssim$10 μm	~150/cm	50 μm	device is triggerable/gatable
Noble Liquid TPC	10^5	10 μ sec	= RT	10 μm	10/cm	1 mm	
Germanium TPC	10^6	10 n sec	50 n sec	?	?	?	mult. scattering potential problem
CCD	$\lesssim 10^3$	10 n sec	Few m sec	5 μm	5-10/cm	15 μm	
Silicon Coupled to CCD	$\lesssim 10^3$	10 n sec	Few m sec	10 μm	100/cm	25 μm	
Negative Electron Affinity Ge (Cesium Oxide Surface)	10^5	Few μ sec*	= RT	1 μm	100-1000/cm	3 μm	device is triggerable/gatable
Field Emission Si	10^5	Few μ sec*	= RT	10 μm	100-1000/cm	30 μm	device is triggerable/gatable
Modified Semiconductor Memory or RAM	?	10 m sec	= RT	10 μm	5 cm	60 μm	very speculative

TABLE III

Typical e^+e^- Collider Beam Pipes

	Beam pipe radius (r_1)	Beam pipe thickness radiation lengths*
CESR	$\gtrsim$5 cm	.004
SLC	1 cm	.001

*(To these values one must add the radiation length for the first silicon detector of 300 μ thickness = .004.)

After some algebra, the extrapolated resolution for the two planes with intrinsic resolution σ_I is:

$$\sigma^2 = \sigma_I^2 \frac{(a^2+1)}{(a-1)^2} + r_1^2 C \qquad (1)$$

The functional dependence of σ upon $a = r_1/r_2$ is shown in Figure 3 as the solid curve, assuming: an intrinsic resolution of $\sigma_I = 10\ \mu$m per silicon detector, a beam pipe radius of 1 cm, and particle momenta of $p \sim 1$ GeV/c (typical for particles produced at the Z^o). The dashed lines in the figure indicate the minimum possible resolution due to multiple scattering in beam pipes - corresponding to the term $r_1^2 C$ which appears in Eqn. (1). For $r_1 = 1$ cm, this is seen to be roughly 10 μm.

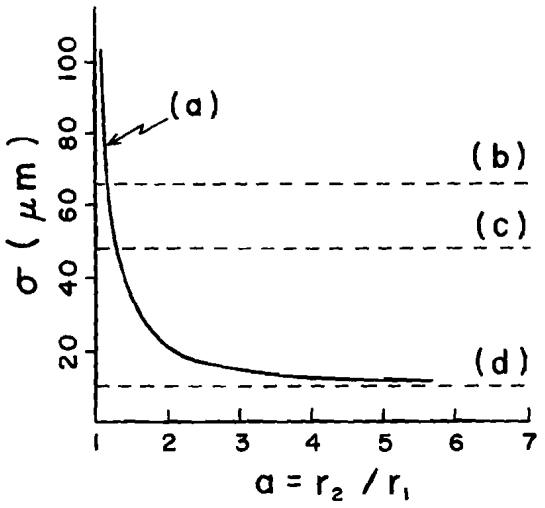

Figure 3. The resolution at an extrapolated decay vertex within the beam pipe in the configuration of Figure 2:
(a) the resolution calculated with Eqn. (1) for a $r_1 = 1$ cm beam pipe;
(b) the resolution lower limit for $r_1 = 5$ cm due to the multiple scattering in the beam pipe and the inner Si detector;
(c) the resolution lower limit for $r_1 = 5$ cm due to the beam pipe alone;
(d) the resolution lower limit for $r_1 = 1$ cm due to the beam pipe alone.

It should be pointed out that Eqn. (1) is a best case and almost certainly underestimates an actual experimental situation because of the following assumptions implicit in the calculation: perfect resolution of the primary vertex; no uncertainties in detector alignment; and no factor for electronic resolution. These factors could easily combine to make the experimental resolution a factor of two larger. Also, the addition of more silicon detectors does not improve the resolution significantly over the two detector case used here.

The subgroup concludes that to look directly for B decays, it is essential to have a very small diameter beam pipe made of low Z material (such as beryllium). The SLC intersection region affords the best chance to satisfy these requirements.

2. Calorimetry

The calorimetry subgroup has concentrated on devices appropriate to the various colliding beam machines. In particular for ep and $\bar{p}p$ colliders, they have considered Fe/shower chamber calorimeters and lead glass arrays (especially extruded lead glass) to be cost effective methods for providing good energy resolution for high energy secondaries. For e^+e^- machines on the other hand, experiments have to cover an enormous dynamic range of energies, $0.1 < E < 50$-100 GeV. Up to now experimenters have had to rely on arrays of NaI crystals to attain the best energy resolution. However recent work with small arrays of $Bi_4Ge_3O_{12}$ (BGO) crystals have indicated that this new material has a number of features which make it preferable to NaI for calorimetric purposes (see the report by S. Herb, et al. in these proceedings). As shown in Table IV, BGO is radiation hard, non-hygroscopic, and has a very short radiation length. Because it is itself a scintillator, it affords excellent energy resolution: $0.3\text{-}1.0/\sqrt{E}$. Tests of a photodiode readout for BGO have been successful, indicating that such detectors can be placed in magnetic fields. Large arrays of BGO are planned for CESR and LEP.

TABLE IV

A Comparison of Properties of Calorimetric Materials

	BGO	NaI	Pb Glass
Radiation Length (X_o) in cm	1.12	2.59	3.2
Density	7.13	3.7	3.61
Resolution	$\frac{0.3 - 1.0}{E^{1/2}}$	$\frac{2\%}{E^{1/4}}$	$\frac{10\%}{E^{1/2}}$
Cost/cc ($)	~15*	2	.052
Cost/X_o^3	21	35	1.7
Radiation Damage	10^6 Rad.	10^4 Rad.	10^3 Rad.

*(Raw material cost is ~ $2/cc; costs for fabrication are expected to drop to ~$5 cc ultimately.)

3. Particle Identification

New techniques in particle identification include: ring-imaging Cerenkov counters, fine-sampling dE/dx detectors, and detectors for transition radiation and synchrotron radiation. This particle identification subgroup considered the first two techniques.

Ring-imaging counters have already been incorporated into existing experiments (E605 at Fermilab is an example). The conventional photosensitive detector is a multi-step chamber containing A-TEA or A-TMAE gas mixtures. These devices have been used successfully in low multiplicity event topologies (1-2 particles), but the real payoff is expected to be obtained in high multiplicity events.

Fine-sampling dE/dx detectors offer the possibility for improved particle identification in the regime of relativistic rise. Shown schematically in Figure 4 is a test device developed at BNL (Ludlam, et al.[1]). A beam of particles is incident onto a drift chamber structure with cathode planes spaced asymmetrically on either side of the readout plane. Output pulses from the anode wires are first shaped and then digitized in 100 MHz ADC's. The output pulses are partitioned into 10 ns samples corresponding to 1/4 mm of A-CO_2 gas. Samples can then be combined into groups of 1, 2, 4, 8, 16, or 64 channels simulating 1/4, 1/2, 1, 4, or 16 mm of gas detector. In Figure 5 is shown the effect of sampling

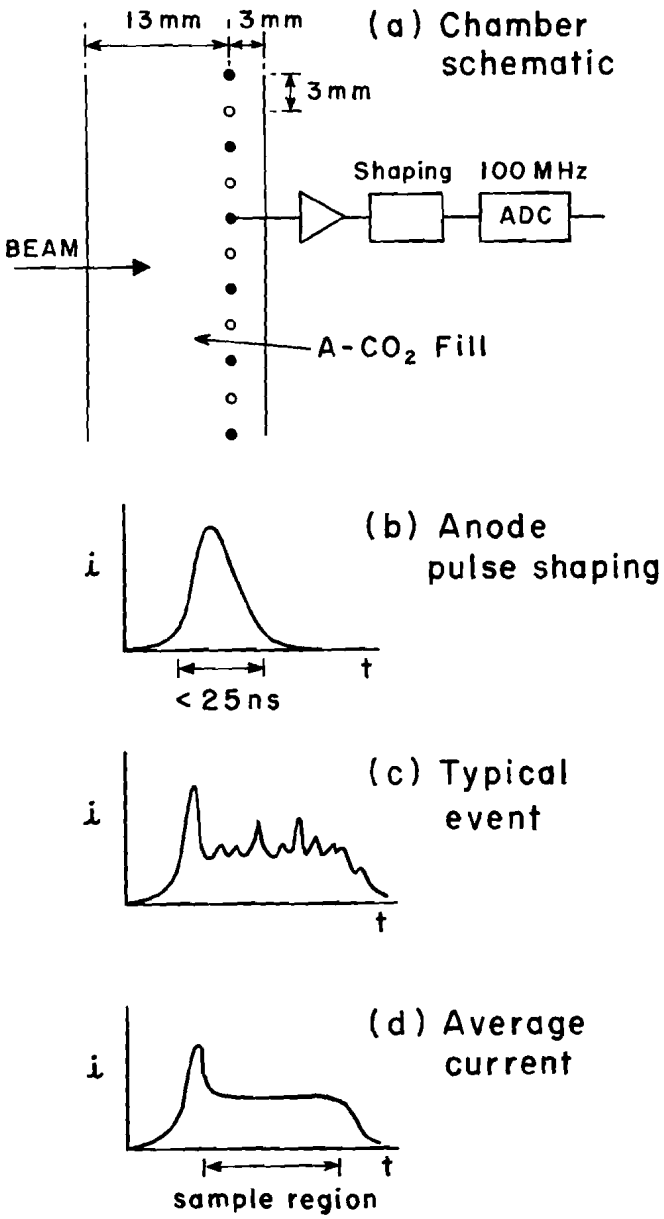

Figure 4. Schematic of a fine sampling drift chamber structure using A-CO_2 gas: (a) chamber geometry; (b) typical shaped anode pulses; (c) typical detected anode current (fluctuations are due to δ-rays); (d) average current at anode wire (bars indicate ADC sampling limits).

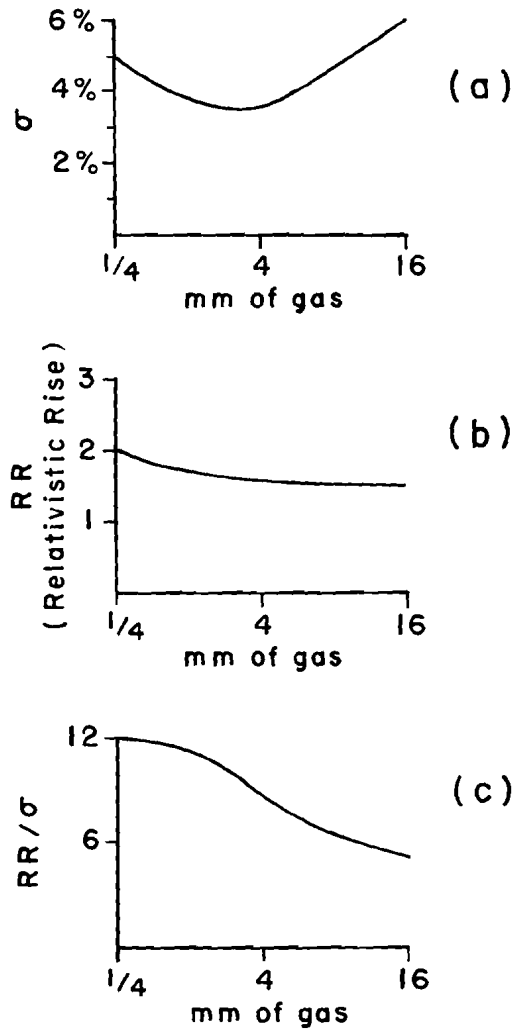

Figure 5. Performance of the fine-sampling drift structure shown in Figure 4 for various sampling sizes of gas: (a) σ of the dE/dx distribution using a truncated mean (see text); (b) the relativistic rise (RR) in dE/dx observed; (c) the ratio of the observed relativistic rise to the width σ. The ratio is clearly enhanced for small sampling sizes.

size on (a) the width σ of the dE/dx distribution, (b) the observed relativistic rise RR = $(E_e-E_p)/E_p$,[2] (c) the ratio RR/σ. A truncated mean method has been used on 1 meter samples and the smallest 50% of the samples have been retained. The ratio RR/σ is seen to increase to a value of ~ 12 for small sampling sizes. This result is roughly a factor of two better than that obtained using conventional ionization sampling (ISIS) techniques for which RR/σ ~ 5.

4. Electrodeless Drift Chambers

This subgroup concentrated on devices which are applicable to very low rate experiments, such as those in deep mine environments. A promising technique for providing inexpensive drift coordinate measurements and ionization information is the so-called "electrodeless" drift chamber shown in Figure 6. Such a structure consists of

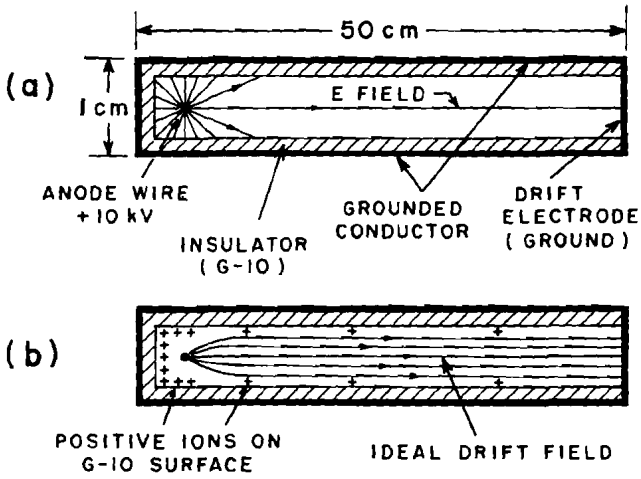

Figure 6. Schematic of an electrodeless drift cell indicating:
(a) the field lines at time t = 0 when the anode wire is placed at +HV;
(b) the field lines at t ~ 10 hrs. later.

a drift cell with an anode wire placed at the center or to one end (see articles by D. Ayres and G. Tzanakos in these proceedings). The walls of the cell are composed of insulator, with the exception of one or two grounded electrodes (cathodes) at the ends of the cell. To operate the device, one simply applies high voltage to the anode wire. Initially very few field lines reach the cathode (Figure 6a). However as cosmic rays traverse the cell, positive ions which drift away from the anode follow the field lines and become implanted on the insulator surface. After ~ 10 hours of cosmic ray "training", the accumulated population of implanted positive ions is distributed in such a way as to make an ideal drift field within the cell (Figure 6b). The simplicity of the technique lends itself to complex and large geometries. One recently documented problem - noted by the Argonne group (D. Ayres) - is that the pulse height observed at the anode wire slowly deteriorates as a function of time. Such problems can arise from overcharging of the insulator surface by positive ions or by non-uniformity and inhomogeneities in the insulator resistivity. It is hoped that this type of difficulty can be eliminated through proper selection of insulating material.

5. High Luminosity Considerations

This subgroup has considered the requirements for electronics and detectors operating in the luminosity range $L \sim 10^{32} - 10^{34}$ cm^{-2} sec^{-1}. A summary of this work appears in the report by E. Platner in these proceedings entitled "High Luminosity Considerations" and we refer the reader to that article for details. To paraphrase the discussion:

1. Primary triggering for high rate experiments will usually involve highly segmented calorimetry.
2. Time resolution for detectors is typically $\lesssim$ 5 n sec, although integrating times can be much longer. This leads to overlaps in events. Segmentation in detection apparatus and the longitudinal displacement of interaction vertices in the beam intersection region assist in alleviating overlap problems.
3. Electronics must be dc coupled or baseline adjusted to prevent pileup difficulties, and detectors must be able to withstand high rates in terms of both efficiency and detector lifetime. Recent experience with drift and proportional wire chambers at ISR, and studies of silicon strip detectors indicate that these devices will operate successfully.
4. The MPS-II detector at BNL was operated successfully in Spring, 1982, in a high intensity beam and serves as a model or "existance proof" of a detector which was designed specifically to handle complicated event topologies in a high rate environment.

The subgroup concludes that luminosities up to 10^{33} cm^{-2} sec^{-1} are handlable with existing technology.

6. Speculative Detector Ideas

In keeping with the Detector Group philosophy of providing a forum for any unusual idea in instrumentation, a number of short presentations were made to the Group at the Workshop. We provide here a list of titles and authors; a number of these topics are included as contributions to these proceedings.

1. Superconducting cavities to detect mass radiation. A. Melissinos
2. Vertex detectors based on (i) negative electron affinity and (ii) field emission semiconductors. R. Lipton

3. A vertex detector consisting of a fiber-optic plate composed of 5 μm diameter scintillating-glass fibers. R. Ruchti
4. BBQ readout of plexipop for fast timing in ν experiments. M. Abolins
5. Innovations in TPC ideas. D. Nygren, H. Sticker
6. A liquid crystal calorimeter. D. Nygren
7. RAM as a vertex detector. R. Thornton
8. A shower detector composed of towers of scintillating glass and heavy glass fibers. R. Ruchti
9. Detection of slow magnetic monopoles using infrared excitation of matter. D. Ayres
10. Channeling of particles in bent silicon crystals. L. Pondrom
11. BGO calorimetry plus photodiode readout. H. Vogel, F. Pauss.

CONCLUSION

Excellent ideas abound in high resolution vertex detection, high resolution calorimetry, particle detection, and in operation of devices in high luminosity environments. With appropriate development of these innovations in instrumentation, we should be able to confront successfully the challenges of physics requiring high luminosity and very high energy.

REFERENCES

1. T. Ludlam, et al., IEEE Transactions on Nuclear Science, Vol. NS28, 439 (1981).
2. E_e is the ionization measured for electrons, E_p is the ionization measured for protons.